

Molecular dynamics simulation of the diffusion behaviour between Co and Ti and its effect on the wear of WC/Co tools when titanium alloy is machined



Dashan Bai^a, Jianfei Sun^{a,b,*}, Wuyi Chen^{a,b}, Daxi Du^a

^a School of Mechanical Engineering and Automation, Beihang University, No. 37, Xueyuan Road, Beijing 100191, China

^b Collaborative Innovation Center of Advanced Aero-Engine, Beijing 100191, China

ARTICLE INFO

Article history:

Received 12 May 2016

Received in revised form

15 August 2016

Accepted 16 August 2016

Available online 19 August 2016

Keywords:

Molecular dynamics

Diffusion

Surfaces

Cutting tools

ABSTRACT

In the process of machining titanium alloy, the high temperature and intensive stress at the tool/chip interface may activate atomic diffusion, which causes the tool to wear. In this paper, the temperature and stress at the interface were investigated using finite-element simulation. The diffusion behaviour of the Co/Ti interface at the atomic level was studied using molecular dynamics simulations. The results show that the cutting speed plays a notably important role in diffusion at the Co/Ti interface. The atomic diffusion across the interface becomes more significant with the increase in cutting speed, and a higher cutting speed corresponds to a thicker diffusion layer. The interfacial region exhibits an amorphous structural order at a high cutting speed; simultaneously, it was easier for the Ti atoms to penetrate into the Co atom side because of the larger interstices among the Co atoms. Turning tests were performed. The element diffusion was analysed based on the Auger electron spectroscopy depth profile. The simulation results were experimentally verified. The microscopic mechanism of the diffusion wear of the tool was revealed. This study contributes to a better understanding of the wear mechanisms of cutting tools in titanium alloy machining.

© 2016 Elsevier Ltd and Techna Group S.r.l. All rights reserved.

1. Introduction

Titanium alloys have been extensively used in aerospace and related engineering fields because of their unique properties such as a high specific strength (strength-to-density ratio) that is maintained at elevated temperatures, high fracture resistance, and good corrosion resistance [13]. They are also attractive candidate materials for sports and biomedical equipment because of their good biocompatibility [3,15]. Despite the increased usage and outstanding qualities, the low thermal conductivity may cause difficulties in heat dissipation during the cutting process. The cutting temperature peak, which is the key factor for the diffusion, appears in the second deformation zone. The extremely high pressure in this area can result in complete contact between the chip underside and the tool rake face. The tool and work surfaces are mechanically interlocked and metallurgically bonded. Therefore, sliding between two surfaces at the immediately bonded regions will not occur, and the macroscopic chip flow along the rake face

introduces severe shear into the bottom layer of the chip [27]. After the workpiece material adheres to the rake face, an element diffusion couple is formed, which may cause a loss of element from the tool and microstructural damage. The schematic diagram of the main diffusion zone in the cutting process is illustrated in Fig. 1. The high temperature and high pressure at the interface significantly affect the element diffusion, which affects the cutting performance of the tool.

Element diffusion between the tool and the workpiece in titanium alloy machining has attracted great interest from the industries and researchers. Numerous studies were performed on tool-workpiece diffusion when titanium alloy is machined. Jawaid et al. [19] reported that the diffusion occurred through the smooth wear regions on the rake face of the tool. Similar results were found by Su et al. [26]. Deng et al. [11] detected the chemical composition in several zones of the tool's worn surface. Elements of the workpiece material were found in the crater wear zone, which demonstrates the existence of diffusion. Armendia et al. [1] also observed the element diffusion by a direct composition analysis on the worn surface. To elaborate the diffusion behaviour, the cutting tools that adhered with the workpiece material were sectioned perpendicularly to the cutting edge in more

* Corresponding author at: School of Mechanical Engineering and Automation, Beihang University, No. 37, Xueyuan Road, Beijing 100191, China.

E-mail addresses: baidashan@126.com (D. Bai), sjf@buaa.edu.cn (J. Sun).

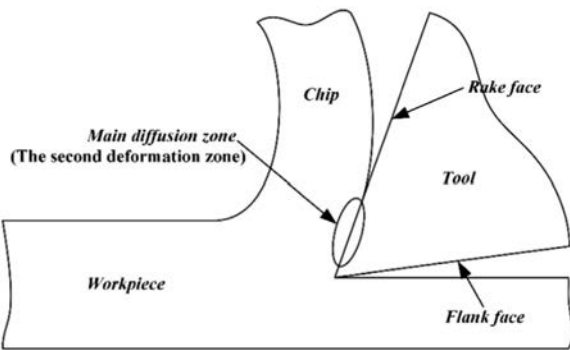


Fig. 1. Schematic diagram of the main diffusion zone in the cutting process.

experiments. The diffusion across the tool/chip interface was generally detected using a line-scanning energy dispersive spectroscopy (EDS) analysis [2,22,14,21].

Although the diffusion behaviour between the tool and the workpiece attracts extensive attention, studies on the diffusion were almost confined to the phenomenon description based on the experimental analysis at the macro level or direct composition detection on the worn surface. Detailed investigations on the diffusion behaviour of the main elements between the cutting tool and the workpiece at the atomic scale during machining and the dynamic characteristics of the diffusion process were rarely reported, and the diffusion mechanism at the interface is not completely clear. Accurate detection of element diffusion across the interface had also scarcely been implemented.

The objective of the present work is to study the diffusion across the Co/Ti interface at the atomic level using molecular dynamics (MD) simulations. The temperature and pressure fields at the tool/chip interface were analysed with the finite-element method (FEM). In the MD simulation process, the atomic diffusion motion can be expressed in a dynamic form. The diffusion features at the interface were investigated in detail. Turning tests were performed at different cutting speeds. The diffusion of various elements across the interface was analysed based on the Auger electron spectroscopy depth profile. The experimental results were used to verify the simulation analysis and demonstrate that the MD simulation to investigate the diffusion of the main elements (Co and Ti) between the tool and the workpiece could reveal the microscopic mechanism of the diffusion wear of the tool. A better understanding of the tool wear mechanisms will facilitate improvement in tool material/structure design and optimization of machining parameters.

2. FEM and MD studies on the atomic diffusion behaviour

2.1. Finite-element simulation of the cutting process

In machining, it is notably difficult to experimentally obtain a detailed 3-D distribution of temperature and stress. Thus, a preliminary finite-element (FE) simulation of cutting was performed using Third Wave AdvantEdge software to analyse the temperature and pressure fields at the tool/chip interface, which are essential to establish the environment of the diffusion regions. To save computing time, the FE simulation of oblique cutting was conducted, which most simplified an actual turning process. The FE simulation model is shown in Fig. 2. The cutting parameters (depth of cut, feed rate, and cutting speed) are listed in Table 1. The temperature and pressure fields on the rake face are shown in Fig. 3. The cutting speed was 120 m/min, the feed rate was 0.05 mm/r, and the depth of cut was 3 mm. The required parameters (see Table 1) to study the diffusion at different cutting speeds are the maximum

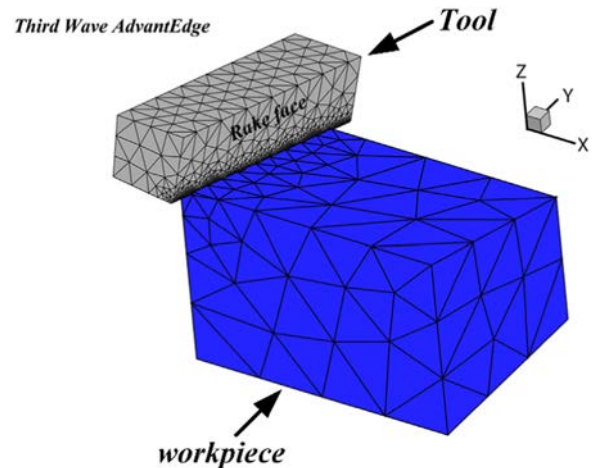


Fig. 2. Model of the FE simulation.

Table 1

Maximum temperatures, pressure, and shear stress at the tool/chip interface at different cutting speeds.

Depth of cut (mm)	Feed rate (mm/r)	Cutting speed (m/min)	Temperature (K)	Pressure (MPa)	Shear stress (MPa)
3	0.05	60	905	1019	330
		80	990	1024	284
		100	1063	1100	187
		120	1142	1167	131

temperature at the tool/chip interface, the average pressure around the location with the highest temperature, and the shear stress at the zone of seizure, where the material movement is actually the plastic shear flow in the chip. Therefore, the resistant force is the plastic deformation force in the shearing process, which should be approximately constant in the seizure zone for a given material when strain hardening is not considered [27] but can decrease with an increase in temperature [25].

2.2. MD simulation modelling and procedure

The WC/Co tools were considered a suitable material to machine titanium alloys [10,18,9]. The Co element, which is a binder in the WC/Co tools, is essential in maintaining the strength of the cutting tools. Co diffusion dominates the crater wear of the tool [17,29]. Ti has the highest content in the titanium alloy (see Table 4). Thus, this study mainly focuses on the diffusion between Co and Ti. In the MD simulation, the inter-atomic potentials play a notably important role. Considerable efforts were made in recent years to develop empirical and semi-empirical models that described many-body potentials. The well-established embedded atomic method (EAM) [16,8] was successfully used to model the elastic properties, defect formation energy, and fracture mechanism of various close-packed bulk metals. The atomic interactions are described by the generalized embedded atom method (GEAM) [30].

First, an MD model about diffusion between Co and Ti was built. In the unit cell, a , b , and c represent three side lengths, and α , β , and γ are the angles between each pair of edges. The space group represents the symmetric relationship of atoms and ions in the crystal structure. Both Ti and Co have a simple hexagonal crystal structure. The sequence number of the space group is 194. The specific parameters in the model are listed in Table 2. The system consisted of Co and Ti slabs, which were put in a simulation box. There was no distance between them. To avoid the

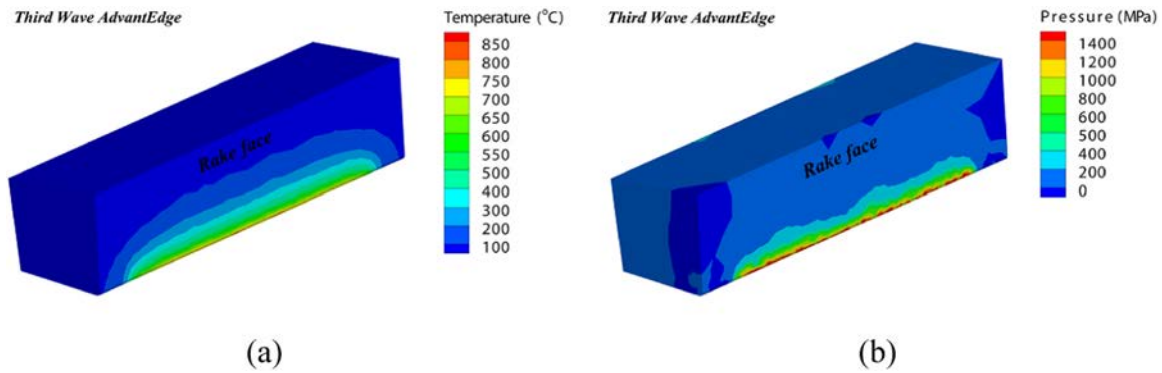


Fig. 3. FE simulation at a cutting speed of 120 m/min, a feed rate of 0.05 mm/r and a depth of cut of 3 mm: (a) temperature field and (b) pressure field.

Table 2
Specific parameters in the model.

Element Name	Crystal Structure	Space Group	Lattice parameters
Ti	Simple Hexagonal	194	a=0.29508 nm b=0.29508 nm c=0.46855 nm $\alpha=90^\circ$ $\beta=90^\circ$ $\gamma=120^\circ$
Co	Simple Hexagonal	194	a=0.25071 nm b=0.25071 nm c=0.40695 nm $\alpha=90^\circ$ $\beta=90^\circ$ $\gamma=120^\circ$

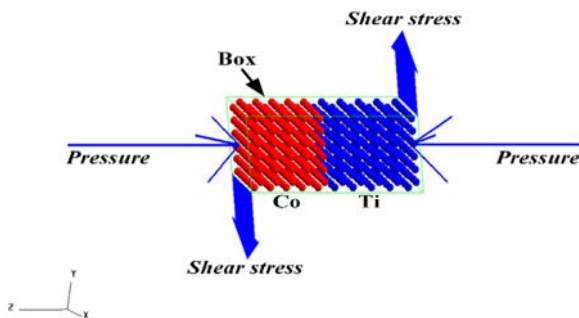


Fig. 4. Schematic diagram of the configuration at the main diffusion zone.

surface effect, periodic boundary conditions in all directions were considered. The initial velocities of the atoms were assumed to follow a Maxwell distribution. Newton's equations of motion for the atoms in the structure were numerically integrated using the Leap-Frog algorithm with a fixed time step of 1 fs. Using a Nose-Hoover thermostat [12], the model was optimized using relaxation at 300 K to keep the system energy steady and the molecular configuration stable. In the relaxation process, an NVT (constant number of particles, constant system volume, and constant temperature) ensemble was used. The time step was set at 2 fs. The length of the run was 5000 steps, and the frame output was every 10 steps. The basic model for further MD simulation was generated. All interfaces were assumed to be ideal crystal planes. Then, the temperatures, pressures, and shear stresses at the tool/chip interface at different cutting speeds, which were obtained from the FEM, were applied to the MD simulation process. The parameters are listed in Table 1. The schematic diagram of the configuration at the main diffusion zone is shown in Fig. 4. In the simulation, an NPT (constant number of particles, constant system pressure, and constant temperature) ensemble was used. The time

step was set at 1 fs. The length of the run was 100,000 steps, and the frame output was every 10 steps.

2.3. Basic algorithm of the diffusion coefficient in the MD simulation

The atoms in the MD simulation perform a non-stop translational motion, where the locations of the atoms vary with time. The mean value of square displacement of a particle is defined as the mean square displacement (MSD) [5] as follows,

$$MSD = \langle |\vec{r}(t) - \vec{r}(0)|^2 \rangle \quad (1)$$

where $\langle \rangle$ is the mean value, $\vec{r}(0)$ is the initial position, and $\vec{r}(t)$ is the location of atom at time t . Eq. (1) shows that the MSD value is the moving activity of a particle. A larger MSD value corresponds to a longer distance that the particle travels in a certain time period.

According to Einstein's diffusion law [7]

$$\lim_{t \rightarrow \infty} \langle |\vec{r}(t) - \vec{r}(0)|^2 \rangle = 6Dt \quad (2)$$

where D is the self-diffusion coefficient.

In the MD simulation, the diffusion coefficient is calculated as follows,

$$D = \frac{1}{6N} \lim_{t \rightarrow \infty} \frac{d}{dt} \sum_{i=1}^N ([r_i(t) - r_{i0}(t)]^2) \quad (3)$$

where N is the number of atoms that diffusively move in the system.

3. Experiments

Turning tests were performed on a CGK6125A CNC lathe, which was manufactured by Beijing GYDCH CNC Machine Tools Works of China (Fig. 5). The combination of a KYOCERA SNGA120408 tool insert in a ZCCCT CSRNR2525M12 tool holder produced the following geometry: rake angle $\gamma_0 = -6^\circ$; clearance angle $\alpha_0 = 6^\circ$; inclination angle $\lambda_s = -4^\circ$; major cutting edge angle $K_r = 75^\circ$. The composition, physical and mechanical properties of the tool inserts are listed in Table 3. The workpiece materials were Ti-6Al-4V in the form of a round bar. The chemical composition and mechanical properties of Ti-6Al-4V are listed in Tables 4 and 5, respectively. Tests were performed with the following parameters: cutting speed $v = 60 - 120$ m/min; feed rate $f = 0.05$ mm/r; depth of cut $a_p = 3$ mm, which were consistent with those in the finite-element simulation (Section 2.1).

During the turning tests, the worn surfaces of the cutting tools were examined using a 3D measuring laser microscope (OLYMPUS,



Fig. 5. Experimental set-up for the turning tests.

Table 3
Properties of the tool inserts.

Composition (wt%)	Density (g/cm ³)	Hardness (GPa)	Fracture toughness (MPa)	Flexural strength (MPa)
WC+6%Co	14.89	16.2	10.1	1446

Table 4
Chemical composition of Ti-6Al-4V alloy (wt%).

Ti	Al	V	O	Fe	Si	C	H
> 89	6.2	4.4	0.18	0.1	0.04	0.01	0.003

Table 5
Properties of Ti-6Al-4V alloy.

Ultimate tensile strength (MPa)	Yield strength (MPa)	Modulus of elasticity (GPa)	Density (g/cm ³)	Thermal conductivity (W/m·K)
1100	1000	110	4.42	6.6

OLS4100) (Fig. 6). To investigate the diffusion of various elements across the interface between the tool material and the workpiece material, the chemical composition variation was detected using Auger electron spectroscopy (AES) (ULVAC-PHI, PHI-700) (Fig. 7), which is a surface analysis technique that uses a high-energy electron beam as the excitation source. The element concentration across the tool-work interface is commonly detected with line-scanning EDS technology, which can generate errors because of a geometric slope at the tool/chip joint and cause wrong energy dispersion readings. The slope is produced in the polishing process on the tool/chip border, which usually exhibits a hardness difference at two sides, whereas AES can eliminate this problem. The qualitative and quantitative results of the surface elements can be

obtained by characteristically analysing the auger electron energy excited by the electron beam. This technique, which is an important surface composition analysis method, can obtain the element distribution state of the material surface along the depth direction via ion-etching technology.

4. Results and discussion

4.1. Discussion about the MD simulations

The relation between the diffusion coefficients of Co and Ti and the cutting speed is shown in Fig. 8. Both diffusion coefficients of Co and Ti atoms increased with the increase in cutting speed. The Co and Ti atoms diffused more significantly when the cutting speed exceeded 80 m/min. Co atoms had a larger diffusion coefficient than Ti atoms at cutting speeds of 60–120 m/min, which indicates that the Co atoms, which escape from the initial position and randomly move around, are more active than Ti atoms in this diffusion model.

The effect of the cutting speed on the diffusion coefficient can be attributed to the increase in temperature and pressure at the interface between the tool and the chip with the increase in cutting speed (see Table 1). According to Arrhenius relationship [24],

$$D = D_0 e^{-Q/RT} \quad (4)$$

where D_0 is the diffusion constant, D is the diffusion coefficient, Q is the activation energy of diffusion, R is the gas constant, and T is the absolute temperature. The diffusion coefficient increases with the increase in temperature. The lattice distortion at the interface becomes more severe when the pressure increases, which strengthens the atomic energy and facilitates the diffusion. Therefore, the atoms easily escape the initial position and randomly move around under the high-temperature and high-pressure conditions.

The atomic diffusion behaviour at different cutting speeds has different features. The configurations of the Co/Ti diffusion interface at different cutting speeds are shown in Fig. 9. When the cutting speed was 60 m/min, the Co and Ti atoms vibrated around the initial position under the action of temperature and stress. Few atoms diffused across the Co/Ti interface, which could be neglected. The thickness of the diffusion layer was notably small (Fig. 9(a)). When the cutting speed was 80 m/min, several Ti atoms began to penetrate into the Co atom side, and only a few Co atoms diffused into the Ti atom side. The Co atom side and the interface exhibited an amorphous structure, whereas the Ti atom side retained a relatively dense structure. The diffusion layer thickness slightly increased at this speed (Fig. 9(b)). The penetration of Ti atoms into the Co atom side intensified, and the Co atoms also began to gradually diffuse into the Ti atom side at cutting speeds of 100 m/min and 120 m/min. Both atom sides and the interface became amorphous, and the diffusion layer thickness increased more significantly at this moment (Figs. 9(c) and (d)).

Figs. 9(a–d) show that the Co atom side and the interface became amorphous first, and the Ti atom side followed with the increase in cutting speed. The interfacial region exhibited an amorphous structural order at high cutting speed, which is consistent with the observation of a similar disordered interface in a Cu–Al system at high temperatures [6]. In the diffusion process, more Ti atoms diffused than Co atoms, and the Ti atoms also travelled longer distances than the Co atoms, which indicated that the Ti atoms more easily penetrate into the Co atom side.

The cutting temperature increased with the increase in cutting speed. The thermal energy accumulated, and the number of vacancies and interstices among the atoms increased. The atomic



Fig. 6. 3D measuring laser microscope.



Fig. 7. Auger electron spectroscopy.

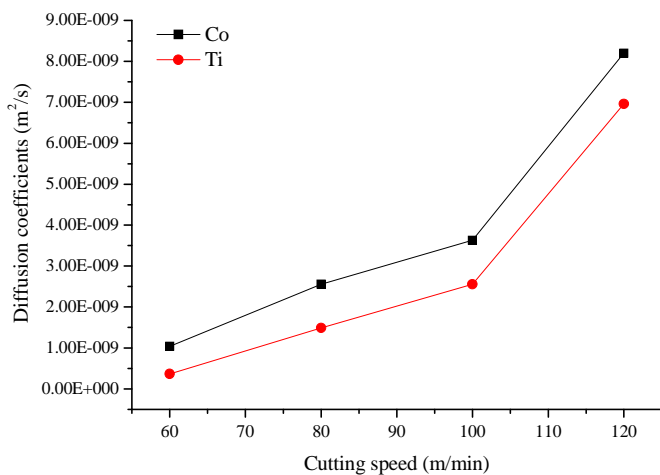


Fig. 8. Curves of the diffusion coefficients of Co and Ti atoms at different cutting speeds.

kinetic energy also increased accordingly, which facilitated the atoms to escape from the initial position and diffuse into one another. Metal atoms are held together through the Coulomb attractive forces between the metal cations and the free valence electrons in the metal crystal. This binding mode is called the

metallic bond whose strength is determined essentially by the number of the valence electrons and the size of the atoms, and generally has a positive correlation with the number of the valence electrons and an inverse correlation with the radius of the metal cation [4,23]. The number of the Co valence electrons is less than that of Ti. Meanwhile, the radius of the Co metal cation is larger than that of Ti. The Co atoms have longer interatomic distances accordingly. Therefore, the strength of metallic bond among the Co atoms is weaker than that among the Ti atoms. The Co atoms more easily escape from the initial position. Thus, the diffusion coefficient of Co atoms is larger than that of Ti atoms in Fig. 8. The Co atoms more easily escape from the original closely-packed position and randomly move. The number of remaining vacancies and interstices among the atoms increases on the side of Co atoms. The Co atom side exhibits an amorphous structure. However, it is more difficult to break the bonds among the Ti atoms than those among the Co atoms because the strength of metallic bond in Ti is larger than that in Co. The Ti atom side largely retained a relatively dense structure, and a few Ti atoms at the interface escaped from the initial position at this time. In general, the interstices among the atoms and the number of remaining vacancies remained small on the Ti atom side when small Ti atoms left the original positions. The large Co atoms were difficult to diffuse into the Ti atom side through the small atomic interstices, and there were few vacancies. The diffusion of Co atoms into the Ti atom side might be hampered by the dense Ti atoms. However, the small Ti atoms at the interface easily penetrated into the Co atom side via the large interstices among the Co atoms, and there were more vacancies (Fig. 9(b)). With the increase in temperature, the number of vacancies of the Co atom side further increased, and the interstices among the Co atoms became larger. The penetration of the Ti atoms into the Co atom side through the interstices and vacancies became more active. Meanwhile, the bonds among the Ti atoms also weakened. The vacancies were likely generated because the Ti atoms left the original position. The interstices among the Ti atoms increased. The Co atoms began to gradually diffuse into the Ti atom side (Figs. 9(c) and (d)). The diffusion of the main elements (Co and Ti) across the interface between the tool material and the workpiece material causes element loss and microstructural damage of the severely stressed tool substrate, which causes tool wear and reduces the tool life.

4.2. Experiment analysis

It is known that the diffusion phenomenon is more remarkable at high cutting speeds. Therefore, in the present work, the AES depth profile was used to analyse the diffusion behaviour at the

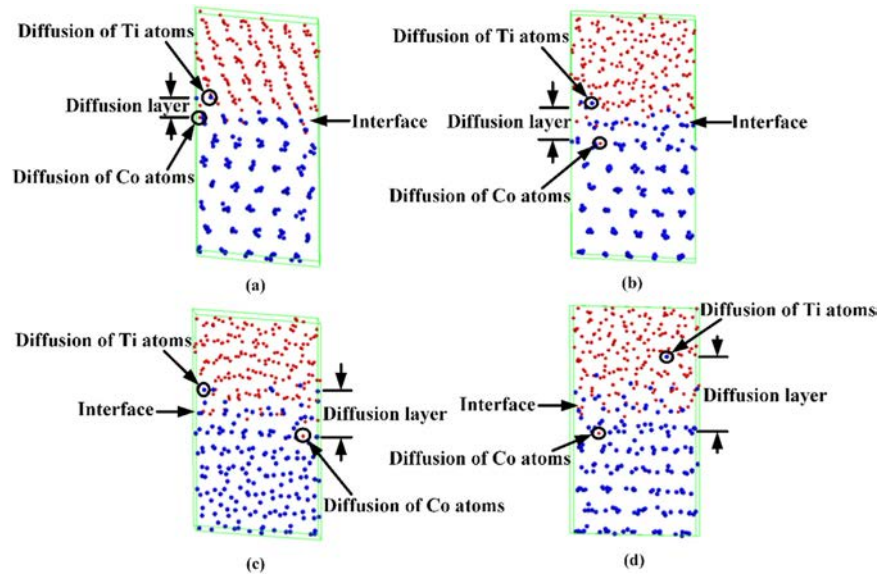


Fig. 9. View of the Co/Ti diffusion interface at different cutting speeds: (a) 60 m/min; (b) 80 m/min; (c) 100 m/min; (d) 120 m/min.

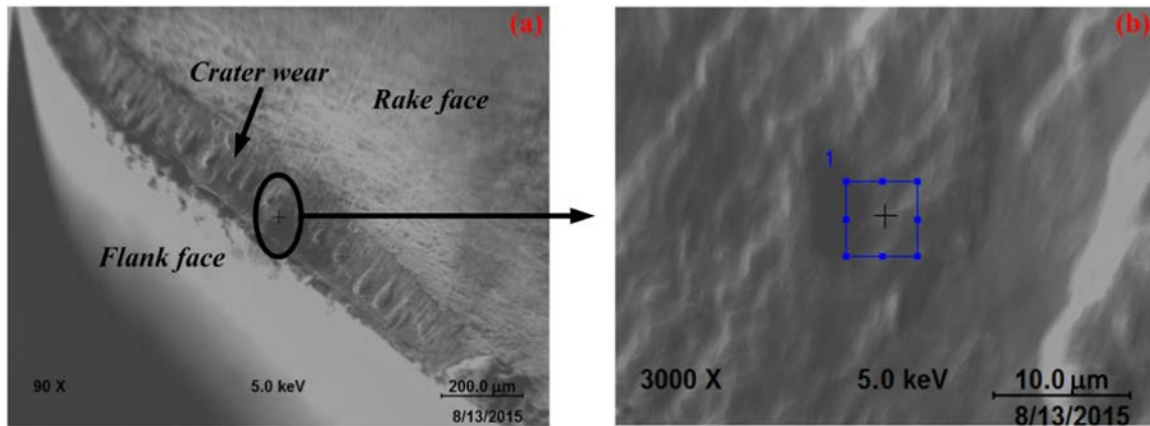


Fig. 10. (a) AES analysis area of the tool wear; (b) enlarged view of the ellipse in the image.

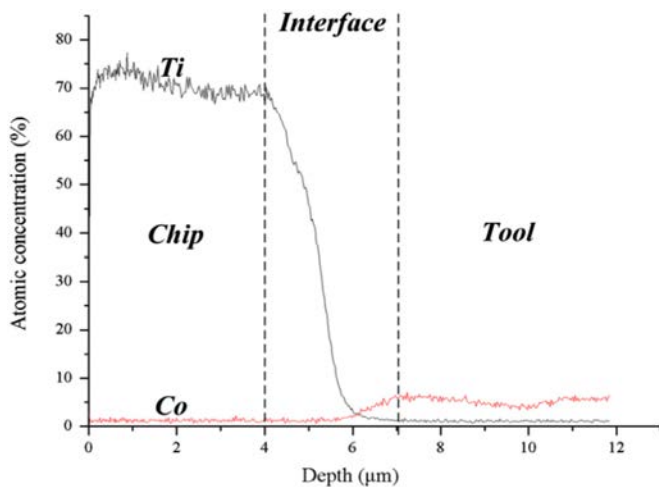


Fig. 11. Depth concentration profiles along the depth direction using the AES surface analysis; the cutting conditions: cutting time=8 min; $v_c=120$ m/min; $f=0.05$ mm/r; $a_p=3$ mm.

highest cutting speed (120 m/min). The analysis area was the lowest position of the crater wear on the rake face of the cutting tool (Fig. 10(a)), where the diffusion should be the most

remarkable because of the high temperature and high pressure. The specific scanning area was a square ($5\ \mu\text{m} \times 5\ \mu\text{m}$) (Fig. 10(b)). The distributed element along the depth direction by the ion-etching technology was obtained. The ionic sputter rate was 30 nm/min. The concentration evolution of the chemical species (Co and Ti) was obtained from the adhered material on the tool surface to some distances in the tool substrate in the depth direction (Fig. 11). Fig. 11 shows obvious gradient distributions of Co and Ti elements at the interface between the tool and the chip, which indicate the diffusion of the Ti element into the Co element side and the diffusion of the Co element into the Ti element side during machining.

In this study, the diffusion distance indicates the diffusion. A longer diffusion distance corresponds to greater diffusion. Fig. 11 shows that Ti had a longer diffusion distance than Co, which indicates that Ti more significantly diffused than Co and that the penetration of Ti atoms into the Co atom side was easier than the penetration of Co atoms into the Ti atom side. This experimental result is consistent with the MD simulation analysis. In addition to the experimental results in this work, the results in the literature are consistent with the MD simulation analysis result [28,20].

The diffusion of the main elements (Co and Ti) between the workpiece and the cutting tool during machining will produce a crater wear on the rake face of the cutting tool. As shown in Figs. 9 (a) and (b), weak diffusions occurred among the Co and Ti atoms at

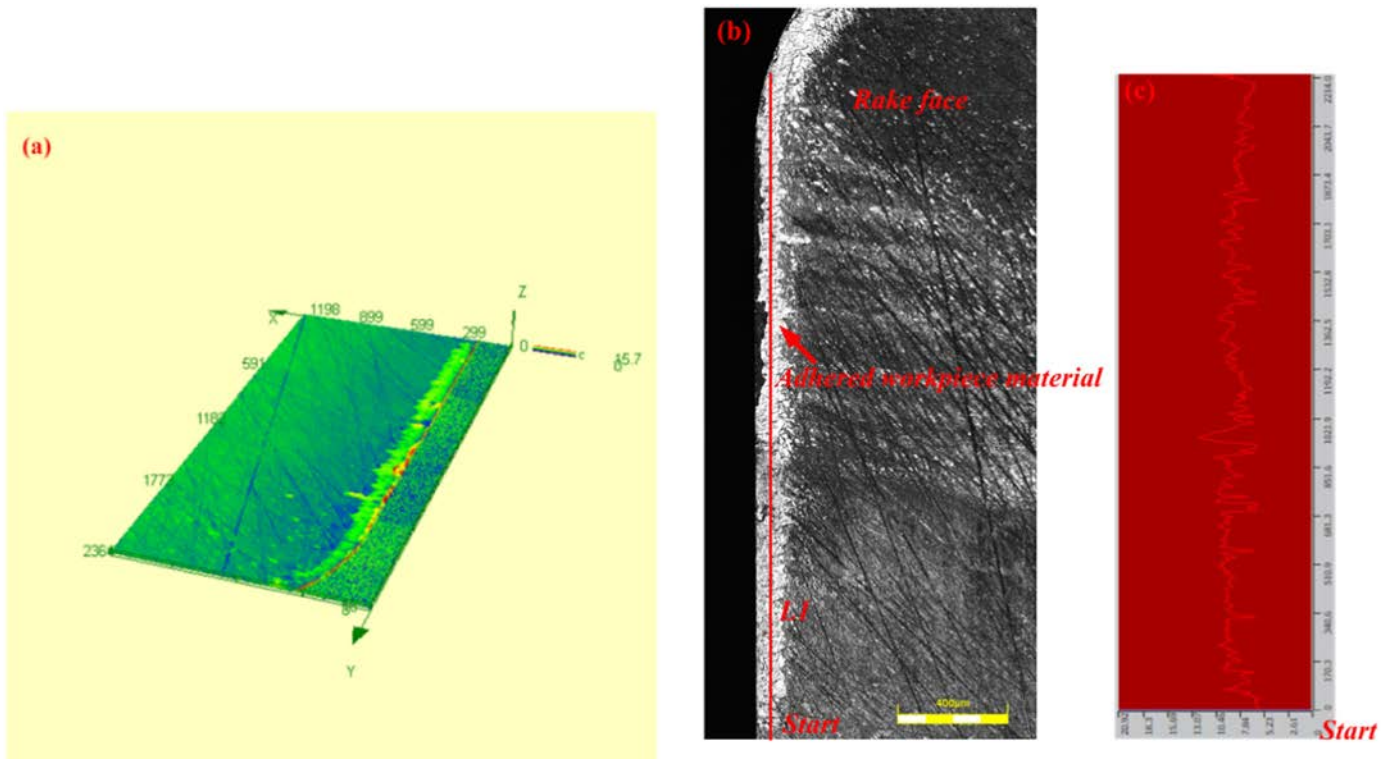


Fig. 12. Observation of the tool rake face under the following cutting conditions: $v=60$ m/min; $f=0.05$ mm/r; $a_p=3$ mm. (a) 3D profile of the rake face by the measuring laser microscope; (b) micrograph of the worn rake face; (c) line profile sectioned along line L1, which was perpendicular to the rake face.

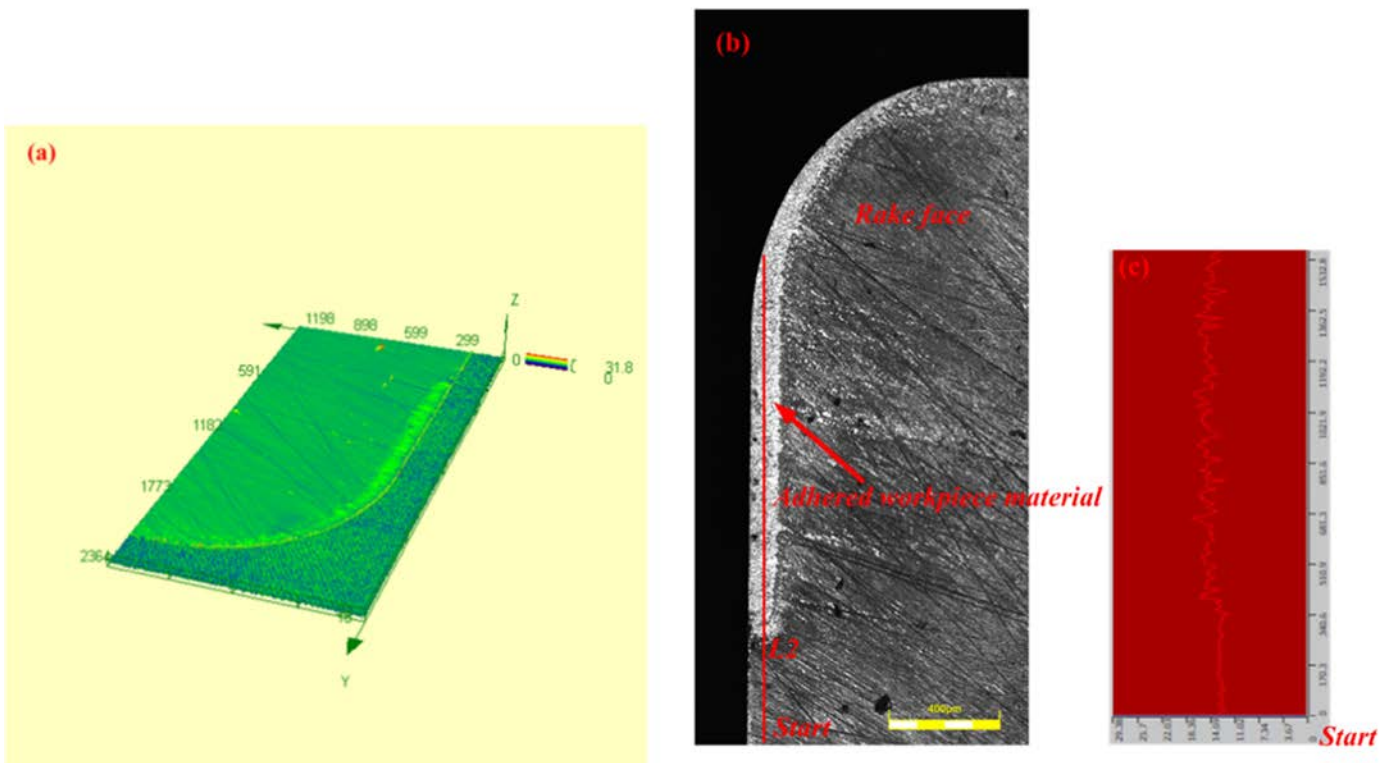


Fig. 13. Observation of the tool rake face under the following cutting conditions: $v=80$ m/min; $f=0.05$ mm/r; $a_p=3$ mm. (a) 3D profile of the rake face by the measuring laser microscope; (b) micrograph of the worn rake face; (c) line profile sectioned along line L2, which was perpendicular to the rake face.

these cutting speeds. The initial surface strength of the cutting tool was almost retained because the loss of the binder element Co and microstructural changes were slight. Thus, there was no visible crater wear when the chip flowed over the rake face of the tool.

The adhesion phenomenon occurred on a large scale at such cutting speeds (Figs. 12 and 13). The average height of the adhered workpiece material, which was measured using a 3D measuring laser micrograph, decreased from $2.86\ \mu\text{m}$ to $1.99\ \mu\text{m}$ when the

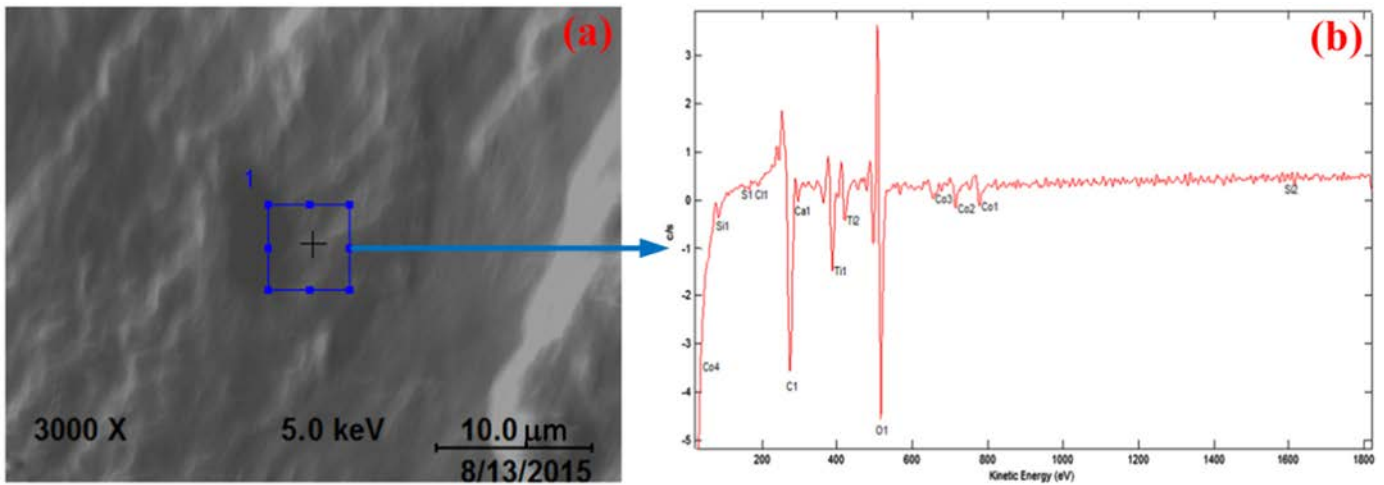


Fig. 14. AES surface analysis of the adhered material on the worn rake face.

cutting speed increased from 60 to 80 m/min.

The maximum temperature at the tool/chip interface and average pressure around the location of the maximum temperature increased when the cutting speed increased (see Table 1). Bright white materials, which contained Ti according to the AES surface analysis (Fig. 14), bonded to the zone of the crater wear on the rake face of the cutting tool. A diffusion couple formed between the workpiece and the cutting tool. Under the high-temperature and high-pressure conditions, the atoms begin to massively diffuse into one another across the tool/chip interface. As illustrated in Figs. 9(c) and (d), the loss of binder atoms Co gradually occurred, which reduced the surface strength of the tool. The compositions changed in the tool surface after many Ti atoms diffused to the Co atom side, which damaged the initial dense

tissue and binders of the tool surface. Subsequently, embrittlement or softening of the tool was likely to occur. At some points, the tool surface, which was weakened by diffusion, was worn off and taken away by the fast flowing chip; then, tool wear occurred (Fig. 15). The maximum depth of the crater wear on the rake face of the cutting tool was approximately 6.85 μm at a cutting speed of 100 m/min for 8 min. One diffusion process finished when the adhering layer was removed from the tool rake face because of the continuous chip flow. Subsequently, a new diffusion process might begin when the workpiece material adhered to the rake face. The aforementioned cyclical phenomenon would cause serious crater wear of the cutting tool, which is more remarkable, particularly at high cutting speed (Fig. 16). The maximum depth of the crater wear on the rake face of the cutting tool was approximately

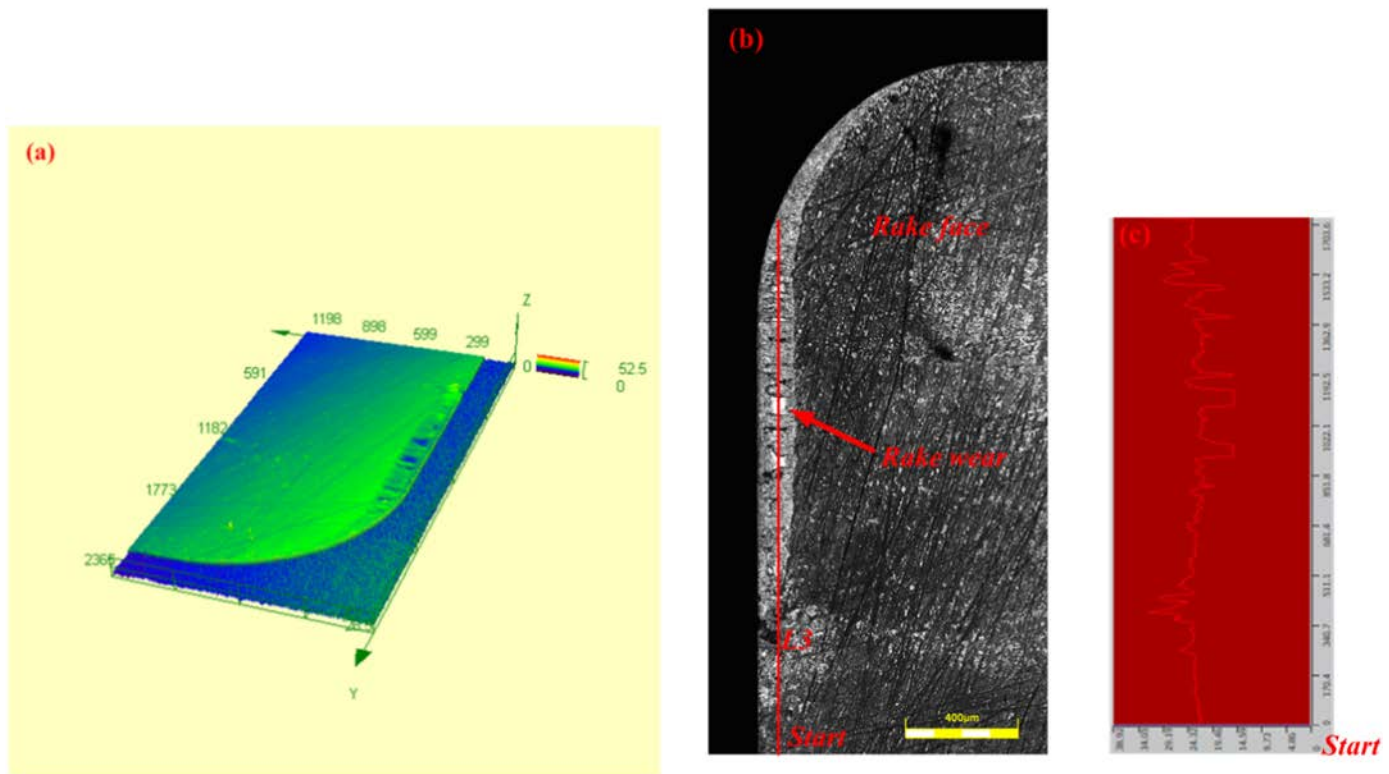


Fig. 15. Observation of the tool rake face under the following cutting conditions: $v = 100$ m/min, $f = 0.05$ mm/r, and $a_p = 3$ mm. (a) 3D profile of the rake face by the measuring laser microscope; (b) micrograph of the worn rake face; (c) line profile sectioned along line L3, which was perpendicular to the rake face.

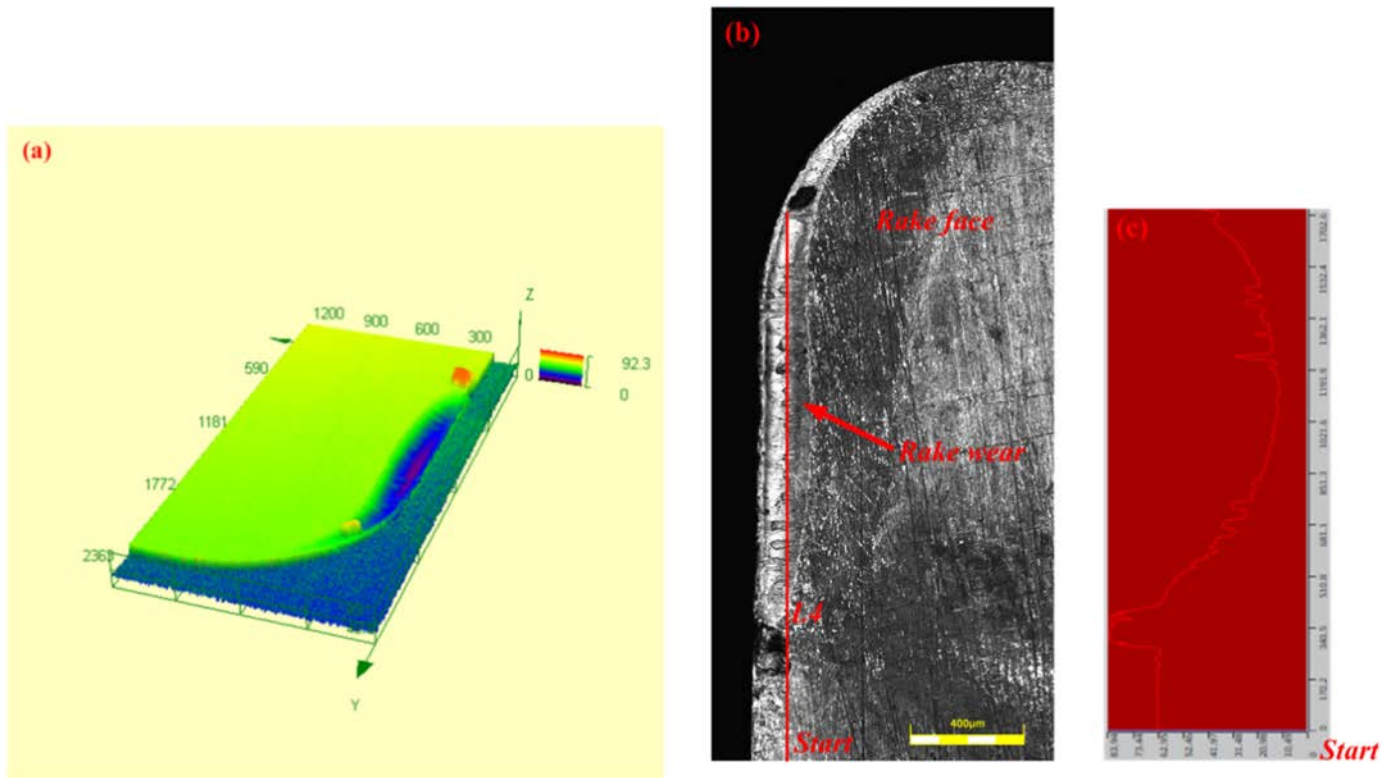


Fig. 16. Observation of the tool rake face under the following cutting conditions: $v = 120$ m/min, $f = 0.05$ mm/r, and $a_p = 3$ mm. (a) 3D profile of the rake face by the measuring laser microscope; (b) micrograph of the worn rake face; (c) line profile sectioned along line L4, which was perpendicular to the rake face.

50.99 μm when the cutting speed was 120 m/min for 8 min.

The experimentally verified MD simulation on diffusion wear can proceed to apply in such research directions as tool material and coating design to delay the diffusion or cutting parameter optimization to work at a suitable cutting temperature. Conventionally, these processes are performed in series cutting tests with massive time and material consumption.

5. Conclusions

The diffusion behaviour of the main elements between the tool and the workpiece at the atomic level was studied using molecular dynamics simulation. The diffusion process at the interface and the microscopic mechanism of the diffusion wear of the tool were revealed. The conclusions are summarized as follows:

1. Based on the comparison between simulation and experimental results, the molecular dynamics simulation was proven to be an effective method to analyse the diffusion of the main elements (Co and Ti) between the cutting tool and the workpiece. The wear mechanisms were analysed at the atomic scale and can be used as a basis for tool material design and cutting-parameter optimization.
2. Co in the cutting tool generally has a more sensitive diffusion coefficient than Ti in the workpiece with the increase in cutting speed.
3. The cutting speed plays a notably important role in the diffusion behaviour between Co and Ti. A higher cutting speed corresponds to a thicker diffusion layer. The interfacial region exhibits an amorphous structural order at high cutting speed.
4. Although Co atoms have a larger diffusion coefficient than Ti atoms, it is relatively easier for the Ti atoms to penetrate into the Co atom side because of the larger interstices among the Co

atoms.

5. The crater wear on the rake face is caused by the diffusion between Co and Ti, which causes the binder loss and damage of the initial dense tissue on the tool surface.

Acknowledgements

This project is supported by the National Natural Science Foundation of China (51305017, 51575029) and the National Major Science and Technology Project (2014ZX04012012).

References

- [1] M. Armendia, A. Garay, L.M. Iriarte, P.J. Arrazola, Comparison of the machinabilities of Ti6Al4V and TIMETAL 54M using uncoated WC-Co tools, *J. Mater. Process. Technol.* 210 (2010) 197–203.
- [2] M.J. Bermingham, S. Palanisamy, M.S. Dargusch, Understanding the tool wear mechanism during thermally assisted machining Ti-6Al-4V, *Int. J. Mach. Tools Manuf.* 62 (2012) 76–87.
- [3] M.J. Bermingham, J. Kirsch, S. Sun, S. Palanisamy, M.S. Dargusch, New observations on tool life, cutting forces and chip morphology in cryogenic machining Ti-6Al-4V, *Int. J. Mach. Tools Manuf.* 51 (6) (2011) 500–511.
- [4] C. Chambers, A.K. Holliday, *Modern Inorganic Chemistry*, 1st ed, Butterworths, London, 1975.
- [5] L. Chen, Y.L. He, W.Q. Tao, The temperature effect on the diffusion processes of water and proton in the proton exchange membrane using molecular dynamics simulation, *Int. J. Comput. Methodol.* 65 (3) (2014) 216–228.
- [6] S.D. Chen, F.J. Ke, M. Zhou, Y.L. Bai, Atomistic investigation of the effects of temperature and surface roughness on diffusion bonding between Cu and Al, *Acta Mater.* 55 (9) (2007) 3169–3175.
- [7] Z.L. Chen, *Molecular Simulation: Theory and Practice* (in Chinese), 1st ed, Chemical Industry Press, Beijing, 2007.
- [8] M.S. Daw, M.I. Baskes, Semiempirical, quantum mechanical calculation of hydrogen embrittlement in metals, *Phys. Rev. Lett.* 50 (17) (1983) 1285–1288.
- [9] P. Dearnley, Understanding the tool wear mechanism during thermally assisted machining Ti-6Al-4V, *Int. J. Mach. Tools Manuf.* (1986) 2699–2712.
- [10] P.A. Dearnley, A.N. Grearson, Evaluation of principal wear mechanisms of cemented carbides and ceramics used for machining titanium alloy IMI 318,

- Mater. Sci. Technol. 2 (1) (1986) 47–58.
- [11] J.X. Deng, Y.S. Li, W.L. Song, Diffusion wear in dry cutting of Ti-6Al-4V with WC/Co carbide tools, *Wear* 265 (11–12) (2008) 1776–1783.
- [12] D.J. Evans, B.L. Holian, The Nose-Hoover thermostat, *J. Chem. Phys.* 83 (8) (1985) 4069–4074.
- [13] E.O. Ezugwu, Z.M. Wang, Titanium alloys and their machinability—a review, *J. Mater. Process. Technol.* 168 (3) (1997) 262–274.
- [14] Y.H. Fan, Z.P. Hao, M.L. Zheng, F.L. Sun, S.L. Niu, Tool diffusion wear mechanism in high efficiency machining Ti6Al4V, *Key Eng. Mater.* 579–580 (2014) 3–7.
- [15] M. Geetha, A.K. Singh, R. Asokamani, A.K. Gogia, Ti based biomaterials, the ultimate choice for orthopaedic implants – a review, *Prog. Mater. Sci.* 54 (3) (2009) 397–425.
- [16] R.W. Hockney, The potential calculation and some applications, *Methods Comput Phys.* 9 (1970) 136–211.
- [17] J. Hua, R. Shivpuri, A cobalt diffusion based model for predicting crater Wear of carbide tools in machining titanium alloys, *J. Eng. Mater. Technol.* 127 (1) (2005) 136–144.
- [18] S.H.I. Jaffery, P.T. Mativenga, Wear mechanisms analysis for turning Ti-6Al-4V —towards the development of suitable tool coatings, *Int. J. Adv. Manuf. Technol.* 58 (5–8) (2012) 479–493.
- [19] A. Jawaid, C.H. Che-Haron, A. Abdullah, Tool wear characteristics in turning of titanium alloy Ti-6246, *J. Mater. Process. Technol.* 92 (1999) 329–334.
- [20] Y.S. Li, Chemical Performance Match Between Cemented Carbide Tools and Ti-6Al-4V Alloy (in Chinese) (PhD thesis), Shandong University, 2010.
- [21] L. Liang, X. Liu, X.Q. Li, Y.Y. Li, Wear mechanisms of WC-10Ni₃Al carbide tool in dry turning of Ti6Al4V, *Int. J. Refract. Met. Hard Mater.* 48 (2015) 272–285.
- [22] M. Nouari, H. Makich, Experimental investigation on the effect of the material microstructure on tool wear when machining hard titanium alloys: Ti-6Al-4V and Ti-555, *Int. J. Refract. Met. Hard Mater.* 41 (2013) 259–269.
- [23] R. Saravanan, M.P. Rani, *Metal and Alloy Bonding: An Experimental Analysis: Charge Density in Metals and Alloys*, Springer-Verlag, London, 2012.
- [24] P. Shewmon, *Diffusion in Solids*, 2nd ed, McGraw-Hill, New York, 1963.
- [25] China Aeronautical Materials Handbook Editorial Board, *China Aeronautical Materials Handbook* (in Chinese), second ed., Standards Press of China, Beijing, 2002.
- [26] Y. Su, N. He, L. Li, X.L. Li, An experimental investigation of effects of cooling/lubrication conditions on tool wear in high-speed end milling of Ti-6Al-4V, *Wear* 261 (7) (2006) 760–766.
- [27] E.M. Trent, P.K. Wright, *Metal Cutting*, third ed, Butterworth-Heinemann, Oxford, 2000.
- [28] Y.F. Yuan, Study on Tool Wear and Cutting Simulation in Machining Titanium Alloy (in Chinese) (PhD thesis), Beihang University, 2010.
- [29] S. Zhang, J.F. Li, J.X. Deng, Y.S. Li, Investigation on diffusion wear during high-speed machining Ti-6Al-4V alloy with straight tungsten carbide tools, *Int. J. Adv. Manuf. Technol.* 44 (2009) 17–25.
- [30] X.W. Zhou, H.N.G. Wadley, R.A. Johnson, D.J. Larson, N. Tabat, A. Cerezo, A. K. Petford-long, G.D.W. Smith, P.H. Clifton, R.L. Martens, T.F. Kelly, Atomic scale structure of sputtered metal multilayers, *Acta Mater.* 49 (19) (2001) 4005–4015.